Atmospheric Environment 133 (2016) 49–59

Contents lists available at ScienceDirect

Atmospheric Environment

journal homepage: www.elsevier.com/locate/atmosenv

Soluble iron dust export in the high altitude Saharan Air Layer

L.M. Ravelo-Pérez [a], S. Rodríguez [b, *], L. Galindo [c], M.I. García [b, c], A. Alastuey [d], J. López-Solano [b]

[a] Research Support General Service (SEGAI), University of La Laguna, Tenerife, Spain
[b] Izaña Atmospheric Research Centre, AEMET, Joint Research Unit to CSIC "Studies on Atmospheric Pollution", Tenerife, Spain
[c] Department of Chemistry, University of La Laguna, Tenerife, 38206, Spain
[d] Institute of Environmental Assessment and Water Research, CSIC, Barcelona, Spain

HIGHLIGHTS

- Soluble iron is observed in the Saharan Air Layer off North African coast.
- Soluble iron occurs in the submicron aerosols in the Saharan Air Layer.
- Enhancement of iron solubility may be linked to dust processing into inner Sahara.

ARTICLE INFO

Article history:
Received 1 July 2015
Received in revised form
9 March 2016
Accepted 11 March 2016
Available online 12 March 2016

Keywords:
Dust
Iron solubility
Fractional iron solubility
Saharan Air Layer

ABSTRACT

Every summer huge amounts of desert dust particles are exported from the hyperarid subtropical Sahara to the North Atlantic the so-called Saharan Air Layer (SAL), a dry, warm and dust-laden corridor that expands from the North African coast (1–5 km.a.s.l.) to the Americas above the marine boundary layer. Because of the potential impact of the dust deposited on the ocean on marine biogeochemistry and climate, we studied the Fe solubility (in seawater) of atmospheric aerosols samples directly collected in the SAL off the North African coast, i.e. the fresh aerosols recently exported from the Sahara in the SAL. The aerosol sampling was performed at ~2400 m.a.s.l. in Izaña observatory in Tenerife island. In the total aerosols, we found low Fe concentrations and high fractional Fe solubility (FFS ~2%) in the North Atlantic free troposphere airflows and high Fe concentrations and low FFS (~0.7%) within the SAL; the resulting FFS versus total dust (or total Fe) plot shows a hyperbolic trend attributed to the conservative mixing of 'fine combustion aerosols' and 'lithogenic mineral dust'. We then focused on the soluble Fe in the SAL. Our results indicate that ~70% of soluble Fe is associated with the dissolution of submicron dust particles, probably involving Fe-bearing clays. We found a FFS of submicron dust (~6%) higher than that typically observed in submicron particles of soil dust samples (<1%). The correlation between FFS and the ammonium-sulphate/dust ratio and the low variability in the Fe/Al ratio in the dust samples, suggests that the increase in the FFS of submicron dust aerosols (with respect to soil dust particles) may be related to the presence of acid pollutants mixed with dust. Previous studies had focused on dust processing and changes of Fe solubility during the trans-Atlantic transport of dust in the SAL. We found that submicron dust exported off the coast of North Africa may have already experienced acid processing over the Sahara, i.e. before dust export to the Atlantic. Export of soluble submicron Fe dust and deposition of coarse and depleted in soluble Fe dust particles during the trans-Atlantic transport may account for the observed variability in dust, soluble Fe and FFS.

1. Introduction

Deposition of airborne soil dust is a major source of iron, phosphorous and other nutrients to the remote ocean that may influence the phytoplankton growth (De Baar et al., 2005). In high-nutrient low-chlorophylic regions, which compose ~30% of the

* Corresponding author.
E-mail address: srodriguezg@aemet.es (S. Rodríguez).

http://dx.doi.org/10.1016/j.atmosenv.2016.03.030

ocean, Fe availability may even limit oceanic primary productivity (Jickells et al., 2005). There is a growing interest about the hypothesis that variability in dust inputs to the ocean may modulate oceanic primary productivity, atmosphere–ocean CO_2 exchange and consequently the Earth's climate (Martin and Fitzwater, 1988). The negative correlation between dust and CO_2 in ice core paleo records suggests that dust-ocean-climate may be subject to important feedbacks (Ridgwell and Watson, 2002) and that increased dust inputs to the ocean may have suppressed CO_2 by 10–20 ppm in glacial versus interglacial periods (Bopp et al., 2003; Rothlisberger et al., 2004).

Knowledge on biogeochemical processes involving dust and its influence on climate is still limited for several reasons. First, the impact of deposited iron on the oceanic biota depends on Fe bioavailability, which can not be directly measured as this is still a poorly understood aspect; measurements of labile/reactive or soluble Fe are being used as a proxy of bioavailable Fe (Fan et al., 2006; Raiswell et al., 2008). Second, there is not a universally accepted (reference) method for measuring iron solubility; methods used in practice (Shi et al., 2012) differ in the extract solvent used (Chen et al., 2006), extraction technique (Wagener et al., 2010) and extraction time (Trapp et al., 2010). Third, the solubility of the Fe bearing dust aerosols depends on dust mineralogy (Shi et al., 2011a) and processes occurring in the atmosphere – before deposition – and in the ocean – after deposition (Baker and Croot, 2010). These, and other limitations on climate research have been discussed in review papers on (i) long term in-situ aerosol dust measurement programs (Rodríguez et al., 2012), (ii) climate relevant physical, chemical and optical dust properties (Formenti et al., 2011; Redmond et al., 2010), (iii) marine biogeochemistry (Schulz et al., 2012), and (iv) on the influence of soil weathering, atmospheric processing and processing occurring in the ocean on iron solubility (Baker and Croot, 2010; Shi et al., 2012).

North Africa is the largest and most active dust source, whose emissions account for 50–70% of global dust emissions (Ginoux et al., 2004, 2012). Dust export occurs in the so-called Saharan Air Layer (SAL), a dry, warm and dust-laden air layer that expands westward from North Africa through the North Atlantic (Prospero and Carlson, 1972). We have focused on the summertime when the SAL (Tsamalis et al., 2013; Rodríguez et al., 2015): (i) is shifted northward linked to enhanced dust emissions in the subtropical Sahara, (ii) is exported at altitudes between 1 and 5 km a.s.l. off the subtropical North African coast (15–30°N) and (iii) results in maximum dust impacts throughout the North Atlantic. During westward transport the SAL shifts downward (down to < 2 km in the Caribbean; Tsamalis et al., 2013) and the aerosol dust population may experience 'aging' by the so-called 'atmospheric processing', a set of processes that may potentially enhance Fe solubility. These processes include (Baker and Croot, 2010; Schulz et al., 2012; Shi et al., 2012): (i) 'acid processing' of dust by reaction with oxidation products of SO_2 and NO_x, (ii) exposure to oxidants and sunlight that may influence dust surface, (iii) in-cloud processing (pass of aerosol through acid-cloud droplets), (iv) evolution from an external to an 'ideally' internal aerosol mixing, and (v) preferential gravitational deposition of large particles. Mixing of dust with combustion (Sholkovitz et al., 2012) and biomass burning (Paris et al., 2010) aerosols may also increase the observed Fe solubility of the resulting aerosol population. Solubility of Fe has been studied in connection to this westward trans-Atlantic SAL movement, e.g. by east-to-west (Baker et al., 2006a) and south-north (Baker et al., 2006b; Buck et al., 2010a,b) cruise measurements, and by collection of samples of 'aged aerosols' of the SAL impacting in the Caribbean (Trapp et al., 2010). A recent global study – which estimated that deposition of soluble Fe on the ocean may have doubled from pre industrial to present times due to combustion emissions of soluble iron and acid processing of dust – found that the highest concentrations of airborne soluble iron are found near North Africa, linked to the desert dust inputs (Ito and Shi, 2016). In this study we have focussed on the solubility of Fe at the beginning of the westward dust corridor–represented by the SAL-that expands from North Africa to the Caribbean. Algae blooms in the Canary Islands have been connected to Saharan dust events (Ramos et al., 2008). In this study we addressed this question: *What are the characteristics of seawater solubility of Fe at the beginning of the North African to Caribbean dust corridor?, i.e. before atmospheric processing potentially occurring during the trans-Atlantic transport may influence dust properties*

The vertical structure of the SAL and the low troposphere of the North Atlantic exhibit some features that should be considered. The dusty SAL expands westward above the marine boundary layer (MBL). The top of this MBL is characterised by the presence of stratocumulus clouds and an inversion layer above them (~1 km.a.s.l.) which hinder vertical mixing processes (Rodríguez et al., 2004), in such a way that sea salt tend to be confined to the MBL, whereas dust concentrations are much higher in the SAL than in the MBL (Prospero and Carlson, 1972). During the westward movement of the SAL, and because of (size dependent) gravitational settling, dust particles move downward from the warm and dry SAL to the cooler and humid MBL where they may experience several processes that may influence Fe solubility, including in-cloud processing, mixing with sea salt and water condensation (with implications on chemical reactions). The comparison of the Fe solubility features of the "fresh aerosols directly collected into the high altitude SAL near North Africa" with those of the "aged aerosols collected in the MBL of the Caribbean and the Western North Atlantic" allows us to assess the role of atmospheric processing during trans-Atlantic transport. In this study we focused on the features of the fresh aerosols recently exported from North Africa, for this reason we collected aerosol samples in the Izaña mountain observatory at ~2400 m.a.s.l. in Tenerife, i.e. directly in the high altitude SAL off the North African coast. As far as we know, these are the first Fe solubility measurements directly in the SAL.

2. Methodology

2.1. Sample collection and aerosol chemistry

The Izaña Global Atmospheric Watch – GAW – observatory (28.309°N, 16.500°W) is located at 2373 m.a.s.l. in Tenerife (Fig. S1 of the Supplementary Material). The site is about 300 km distant to the coast of North Africa; according to the back-trajectories an air parcel may take between 15 and 20 h to travel from the North African coast to Izaña. From 12 to 19 August 2011, we collected aerosol (particulate matter – PM_x) samples in four size fractions: total particulate matter (PM_T) and particulate matter with an aerodynamic diameter smaller than 10, 2.5 and 1 μm (PM_{10}, $PM_{2.5}$ and PM_1, respectively). Sampling was performed in quartz micro-fiber filters (30 m^3/h) at night (22:00 to 06:00 GMT), when upslope winds – that could transport air masses from the boundary layer – have ceased and Izaña is exposed to free troposphere airflows. We refer to samples collected from 22:00 GMT (day D-1) to 06:00 h of day D, as day D. Every night we simultaneously collected samples of PM_T, PM_{10}, $PM_{2.5}$ and PM_1 in different samplers. Thus, a total of 27 PM_x samples were collected along 7 consecutives nights (13–19 August 2011): 7 samples of PM_T, 7 of PM_{10}, 6 of $PM_{2.5}$ and 7 of PM_1. $PM_{2.5}$ was not sampled on the 17 of August 2011 due to sampler failure. Concentrations of PM_x were determined conditioning the filters (before and after sampling) at 20 °C and 30–35%RH and applying the gravimetric method following the EN14907 protocol (except for RH which was set to 30–35% instead of 50%).

The GAW aerosol chemical composition program at Izaña includes: i) elemental composition by ICP-AES and ICP-MS analysis, ii) $SO_4^{=}$, NO_3^{-} and Cl^{-} by High Performance Liquid Chromatography, iii) NH_4^{+} by ion selective electrode and iv) organic carbon and elemental carbon by thermo optical transmittance (see details in Rodríguez et al., 2011). The standard-operation-procedure includes analysis of blank field filters and reference materials. We determined the concentrations of dust as the sum of Earth crust components (Al, Fe, Ca…) normalized in such a way that Al accounts for 8% of dust (see details in Rodríguez et al., 2012); this Al normalization allows comparisons with other studies (e.g. Trapp et al., 2010). Chemical composition is included in section S1 (Table S1) of the Supplementary Material. Table 1 (discussed below) shows the mean chemical composition and mass closure of PM_x during part of the campaign; the undetermined fraction of the aerosol mass – i.e. difference between the gravimetric PM_x concentrations and the sum of the determined species – is much higher in PM_1 than in the other PM_x components. This is attributed to (1) lower accuracy of the gravimetric technique at the usual low PM_1 concentrations, compared to PM_{10} and PM_T, and (2) the fact that water was not determined and the more hydrophilic species tend to occur in the submicron fraction (e.g. ammonium sulphate), whereas the coarse and supercoarse fractions are dominated by less hydrophilic mineral dust. The fact that nitrate is observed in the coarse fraction whereas ammonium occurs in the fine fraction was use to split sulphate in two components based on stoichiometry (see details in Rodríguez et al., 2011): (1) ammonium–sulphate (a-$SO_4^{=}$) and (2) non ammonium–sulphate (na-$SO_4^{=}$).

2.2. Soluble iron

This section includes the key points of the method we used for measuring Fe solubility in sea water at the pH measured in the ocean of the study region; details are provided in section S2 of the Supplementary Material. We determined Fe solubility at pH = 8.13 in all PM_x samples and at pH = 4.7 (adjusted with 2.0 M HNO_3) in a selected set of PM_x samples. This allows us to assess how Fe solubility changes with pH and facilitates comparisons with other studies that measured Fe solubility at pH values of about 4.7 (Baker and Jickells, 2006; Baker et al., 2006a,b; Chen and Siefert, 2004; Shi et al., 2011b), including pHs ~3.5 for studying in-cloud processing (Shi et al., 2012) and <2 for studying acid processing (Nenes et al., 2011).

Because Fe concentrations in seawater are low (Millero and Sohn, 1992) and the saline composition may result in a high background signal (Bermejo-Barrera et al., 1998), sensitive and selective analytical techniques as well as preconcentration methods were used. Moreover, Fe solubility is strongly dependent on pH and the used extract/solvent (Shi et al., 2012). Thus, we developed a method based on the application of an optimized solid-phase extraction (SPE) procedure with 8-hydroxyquinoline (8-HQ) as an organic chelating reagent, which forms uncharged iron complexes, and subsequent analysis by graphite furnace atomic absorption spectrometry (GAAS).

The optimized method for the extraction of the aerosol samples, preconcentration and soluble Fe measurement followed these steps: seawater was collected, filtered and pH was measured or adjusted, as appropriate. Then, a piece of filter with the aerosol sample (6.25 cm^2) covered with 25 mL of seawater at pH 8.13 in a 50 mL polypropylene tube, was capped, shaken and sonicated for 20 min and then allowed to stand overnight. Subsequently, the piece of filter was removed and the seawater sample was filtered and mixed with 25 μL of 0.5 M 8-HQ solution. Afterwards, pH was adjusted to 7.5 ± 0.1 by addition of 5.0 M ammonia solution and sample was passed through a C_{18} SPE cartridge previously washed with 2.0 M HNO_3 and Milli-Q water, activated with metanol and Milli-Q water and conditioned with 0.01 M ammonium acetate (pH 7.0). After that, 0.01 M ammonium acetate was rinsed and the cartridge was dried under vacuum. The elution was carried out with 2.0 M HNO_3 and the eluted iron were measured after dilution with Milli-Q water (1:39) by GAAS.

The whole method was validated in terms of linearity (calibration curves at five levels of concentration), precision (repeatability assessed by analysing three times the same sample), recoveries (spiking at three different concentration levels) and limit of detection, LOD (calculated using 3σ of the blank and an air volume of 240 m^3), which provided satisfactory results ($r^2 > 0.995$, relative standard deviations percentages (RSD) lower than 9.3%, recoveries higher than 95% and atmospheric LOD of 91 pg/m^3). For the calculations of the iron solubility, concentrations in extracts were converted into atmospheric concentrations by calculating the total quantity of analyte on each filter, after appropriate (procedural and operational) blank correction and dividing by the known volume of air filtered for each sample.

Fig. 1A and B shows concentrations of soluble (sol) Fe at pH 4.7 versus those obtained at pH 8.13. Soluble Fe concentrations at both pH show high linearity ($r^2 > 0.98$), the values at pH 4.7 are 26% higher in the PM_{10} and 21% higher in the $PM_{2.5}$ particles with respect to the values at pH 8.13. At both pHs, the fractional Fe solubility (FFS) – i.e. concentrations of soluble Fe divided by total Fe – versus total Fe plots show the hyperbolic trend (Fig. 1C–D) observed in global scale data sets (Sholkovitz et al., 2012).

Table 1
Chemical composition of PMx (14–18 August 2011) in the Saharan Air Layer, including a mass closure (A) and concentrations of some key elements (B).

A)	PM_T		PM_{10}		$PM_{2.5}$		PM_1	
	μg/m³	%	μg/m³	%	μg/m³	%	μg/m³	%
PM_x	119.9		117.1		39.8		17.9	
∑ components	115.6	96.5	110.7	94.6	35.5	89.2	10.7	60.0
Undetermined	4.2	3.5	6.4	5.4	4.3	10.8	7.1	40.0
Dust	111.1	92.7	107.7	91.4	33.3	83.8	9.5	53.0
a-$SO_4^{=}$	0.60	0.5	0.60	0.5	0.61	1.5	0.62	3.5
NH_4^{+}	0.20	0.2	0.21	0.2	0.21	0.5	0.22	1.3
NO_3^{-}	1.11	0.9	1.07	0.9	0.36	0.9	0.01	0.0
OC	1.83	1.5	1.23	1.1	0.71	1.8	0.32	1.8
EC	0.02	0.0	0.02	0.0	0.02	0.1	0.03	0.1
Traces	0.80	0.7	0.61	0.5	0.25	0.6	0.06	0.4
B)	μg/m³		μg/m³		μg/m³		μg/m³	
na-$SO_4^{=}$	2.68		2.64		1.09		0.07	
Al	8.91		8.77		2.82		0.76	
Ca	3.95		3.32		0.89		0.16	
Mg	1.77		1.56		0.50		0.13	
Fe	4.54		4.14		1.34		0.38	
K	1.96		2.02		0.14		0.15	
V	13.67		12.23		4.28		1.70	
Ni	4.16		3.29		1.34		0.90	

2.3. Complementary data

We used Aerosol Optical Depth data from the dark target and deep blue products of the MODIS instrument onboard the Aqua satellite (Levy et al., 2010; Hsu et al., 2013) and 10 days FLEXTRA back trajectories (Stohl, 1999) for detecting the Saharan Air Layer and studying the origin of the air that reached Izaña observatory (Fig. 2). The daily, 1 × 1 degree, MODIS-Aqua data (level 3, collection 5.1) were downloaded from the Giovanni online data system. FLEXTRA back trajectories were calculated using ECMWF data. The average value was calculated and plotted in those pixels where both dark target and deep blue MODIS products were available.

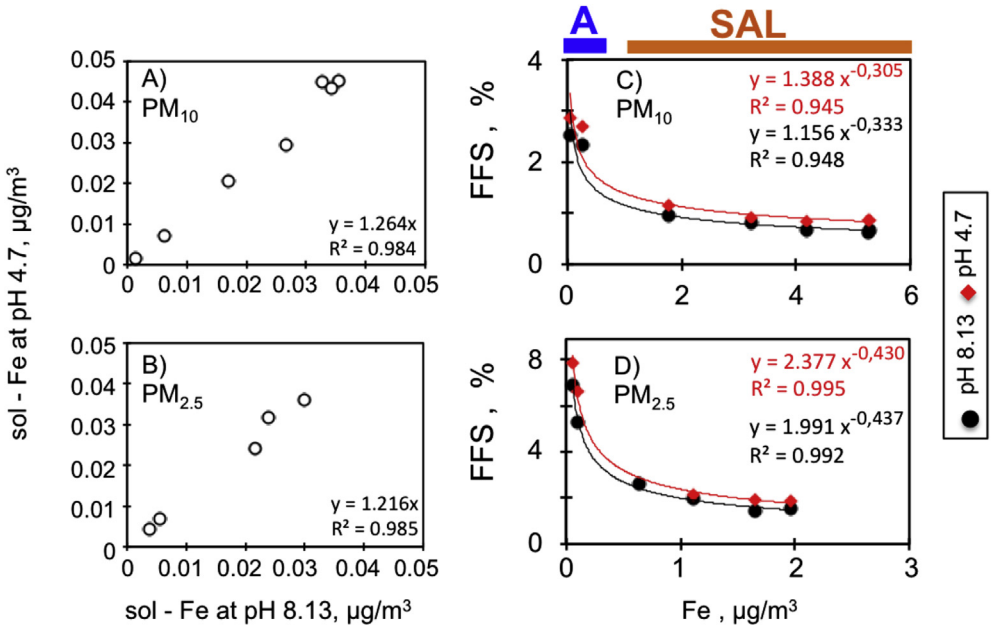

Fig. 1. Concentrations of soluble (sol) Fe at pH 4.7 versus at pH 8.13 in PM_{10} (A) and $PM_{2.5}$ (B). Fractional Fe Solubility (FFS) at pH 4.7 and at pH 8.13 versus Fe concentrations in PM_{10} (C) and $PM_{2.5}$ (D). Samples collected in the Saharan Air Layer (SAL) and under Atlantic airflow conditions (A).

3. Results and discussion

3.1. Dust events and soluble iron

Fig. 2A shows the time series of total dust ($dust_T$) concentrations at Izaña during August 2011. We used Aerosol Optical Depth (AOD) data satellite observations (Fig. 2B–D) and back-trajectories (Fig. 2B–D) for detecting the SAL and studying the origin of the air that reached Izaña. In August, the SAL typically occurs between 15°N and 30°N off the North African coast (Rodríguez et al., 2015). The presence of the SAL results in dust impacts and low visibility in Izaña (3B), whereas shifts of the SAL south of Tenerife are regularly associated with western Atlantic airflows and pristine air at Izaña (Fig. 3A).

The soluble Fe study was performed during 13–19 Aug 2011 (Fig. 2A). On the 13 of August 2011 low $dust_T$ (<5 µg/m^3) concentrations were associated with Atlantic airflow conditions (Fig 2B and E). From 14 to 18 August, the SAL expanded northward (Fig. 2C and F) resulting in high $dust_T$ concentrations at Izaña (60–170 µg/m^3; Fig. 2A). The ochre colour of the aerosol samples evidences that the aerosol mass was dominated by desert dust (Fig. 3C); this is supported by the PM_x mass closure (Table 1, discussed below). The back-trajectories for this event (14–18 Aug 2011) show transport of dusty air from a region – at the north of the Inter-Tropical Convergence Zone – which expands from Central Algeria through Northern Mauritania and Western Sahara (Fig. 2F). Rodríguez et al. (2015) showed that summer-to-summer variability in dust concentrations at Izaña is associated with north-south shifts of the SAL connected to variability in the intensity of winds in this region that they denoted Subtropical Saharan Stripe. On the 19 of August 2011, western Atlantic airflows prevailed, resulting in low $dust_T$ concentrations (13 µg/m^3) at Izaña (Fig. 2A, D and G).

Fig. 4A shows time series of $dust_T$ and total soluble iron (sol-Fe_T) concentrations. In Izaña, sol-Fe_T tracked $dust_T$ concentrations. A similar dust tracking by sol Fe was observed – connected to the SAL impacts – by Trapp et al. (2010) in Barbados. Cruise measurements also found a correlated increase in dust and sol Fe concentrations when crossing north-to-south the MBL impacted by the SAL in the Central North Atlantic (Buck et al., 2010a). The values of the fractional Fe solubility for total Fe (FFS_T: soluble iron / total iron, in %) we observe during dust events at Izaña, ranging between 0.50 and 0.85% (at pH = 8.13), are close to those measured during Saharan dust events in the Mediterranean (0.5% at pH = 8; Theodosi et al., 2010) and the North Atlantic (~0.5%; Sedwick et al., 2007).

3.2. Fe solubility and particle size

Fig. 4 includes time series of dust concentrations (dust), soluble iron (sol Fe) and fractional Fe solubility (FFS) in the four studied size fractions (total, < 10 µm, < 2.5 µm and <1 µm): $dust_x$ ($dust_T$, $dust_{10}$, $dust_{2.5}$ and $dust_1$), sol-Fe_x (sol-Fe_T, sol-Fe_{10}, sol-$Fe_{2.5}$ and sol-Fe_1) and FFS_x (FFS_T, FFS_{10}, $FFS_{2.5}$ and FFS_1). The tracking of dust by soluble Fe is observed in the four cut-size fractions in such a way that the highest sol-Fe_{10}, sol-$Fe_{2.5}$ and sol-Fe_1 levels were also recorded in the SAL (Fig. 4B–D), as previously described for sol-Fe_T (Fig. 4A).

Fig. 5A shows the FFS_T versus $dust_T$ concentrations. Baker and Jickells (2006) argued that this inverse – hyperbolic – relationship between FFS and aerosol mass suggests that total iron solubility is influenced by the variability in particle size during atmospheric transport due to deposition of large particles and by the atmospheric processing of the smaller particles. Shi et al. (2011b) found that FFS of fine Saharan dust particles of soil samples (FFS = 0.2–0.8% for <1 µm particles) was just slightly higher than that of coarse dust particles (FFS = 0.1–0.3% for >1 µm particles), and significantly lower than those observed in aerosol dust samples collected in the North Atlantic (e.g. those observed in this study); they concluded that deposition of coarse dust particles alone is unlikely to be an important factor in the observed inverse relationship between FFS and dust concentrations, and that atmospheric processing and/or mixing of dust with combustion particles are probably the main mechanisms to cause the increased iron solubility observed in the long-range transported dust aerosols. We observe that high FFS_T were recorded under the low aerosol conditions linked to western Atlantic airflows, whereas low FFS_T were recorded under high $dust_T$ conditions in the SAL (Fig. 5A). In the subtropical Western North Atlantic, Sedwick et al. (2007)

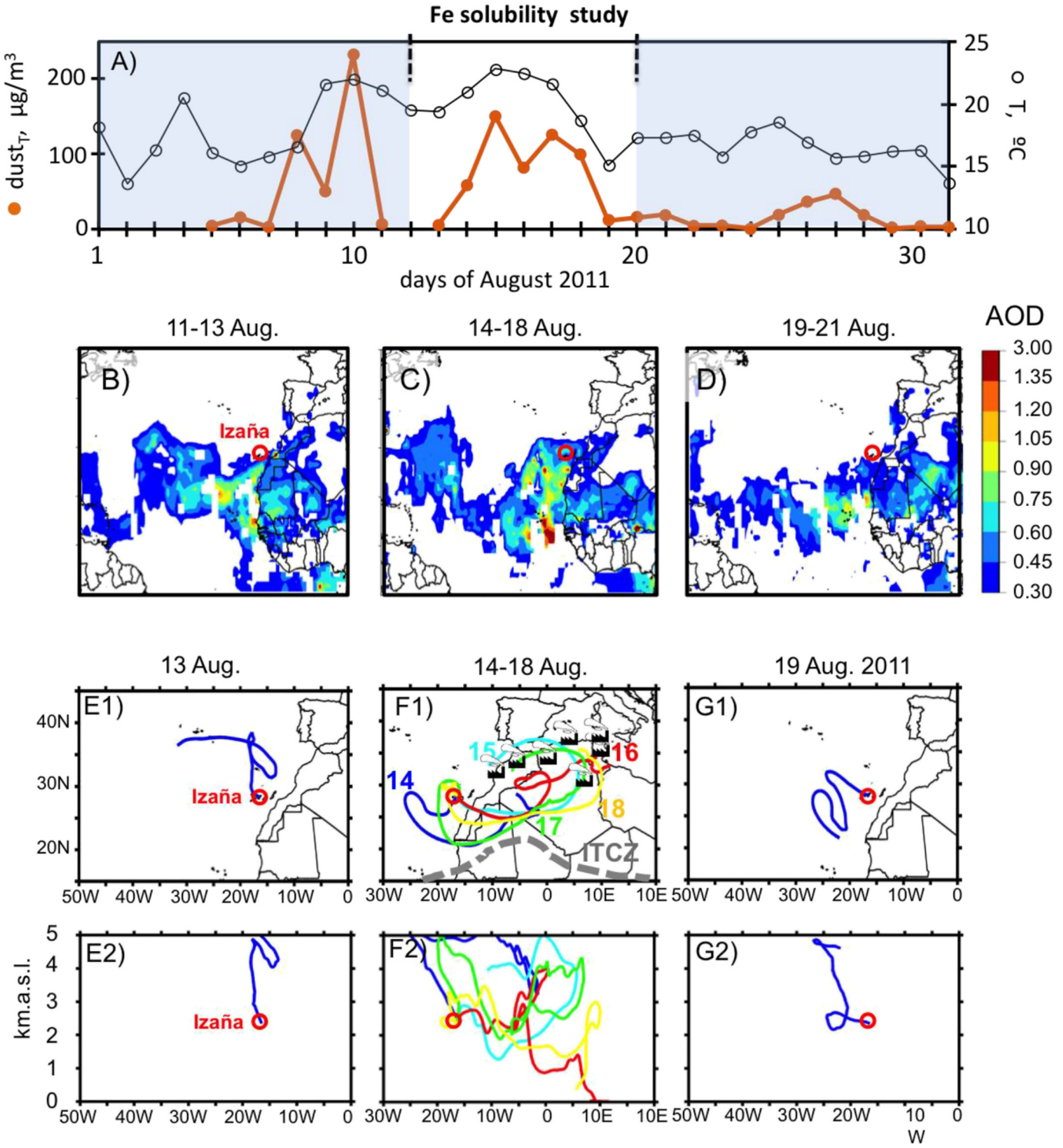

Fig. 2. A) Daily concentrations of dust$_T$ and temperature at Izaña in August 2011. Mean Aerosol Optical Depth (MODIS) averaged before (B, 11–13 Aug 2011), during (C, 14–18 Aug 2011) and after (D, 19–21 Aug 2011) the study dust event. Horizontal (E1–G1) and vertical (E2–G2) components of 10 days back-trajectories arriving to Izaña (black circle). Industrial areas of Morocco, Algeria and Tunisia -according to Rodríguez et al. (2011)- is indicated in F1. Location of Izaña observatory is highlighted with red circle.(For interpretation of the references to colour in this figure legend, the reader is referred to the web version of this article.)

described this hyperbolic relationship between FFS and total Fe in terms of mixing of two types of aerosols: Saharan dust (which resulted in high Fe concentrations and low FFS ~0.45%) and combustion aerosols from North America (very low Fe concentrations and high FFS ~20%). Subsequently, Sholkovitz et al. (2012) found that this mixing of 'lithogenic' mineral dust (high Fe with low FFS) and non-lithogenic 'combustion' fine aerosols (low Fe with high FFS) accounted for the observed hyperbolic relationship between FFS and total iron in regional and global scales.

We observed a strong dependence of Fe solubility on particle

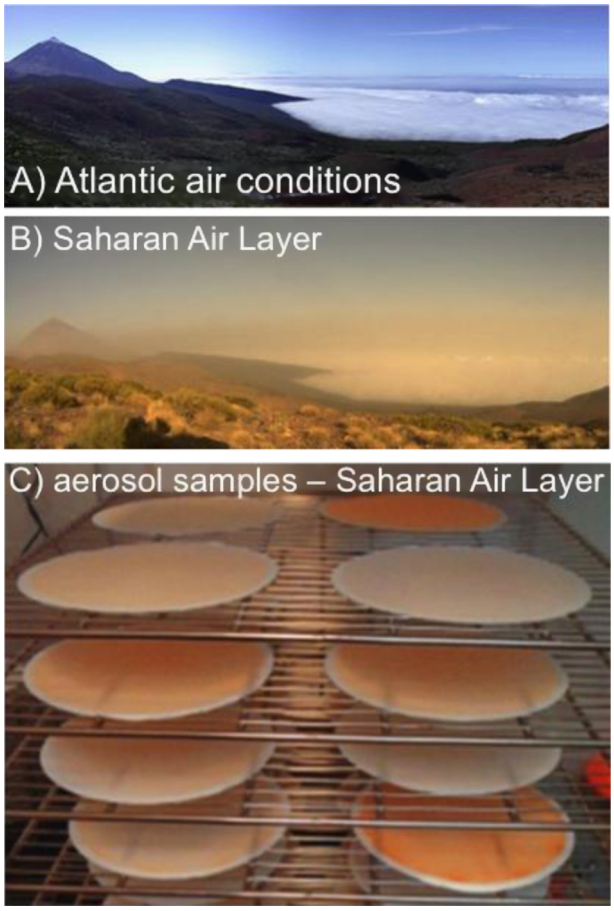

Fig. 3. View from Izaña observatory to NW (Teide volcano) under (A) Atlantic airflow and (B) Saharan Air Layer conditions. (C) Batch of PM_x samples collected in the Saharan Air Layer.

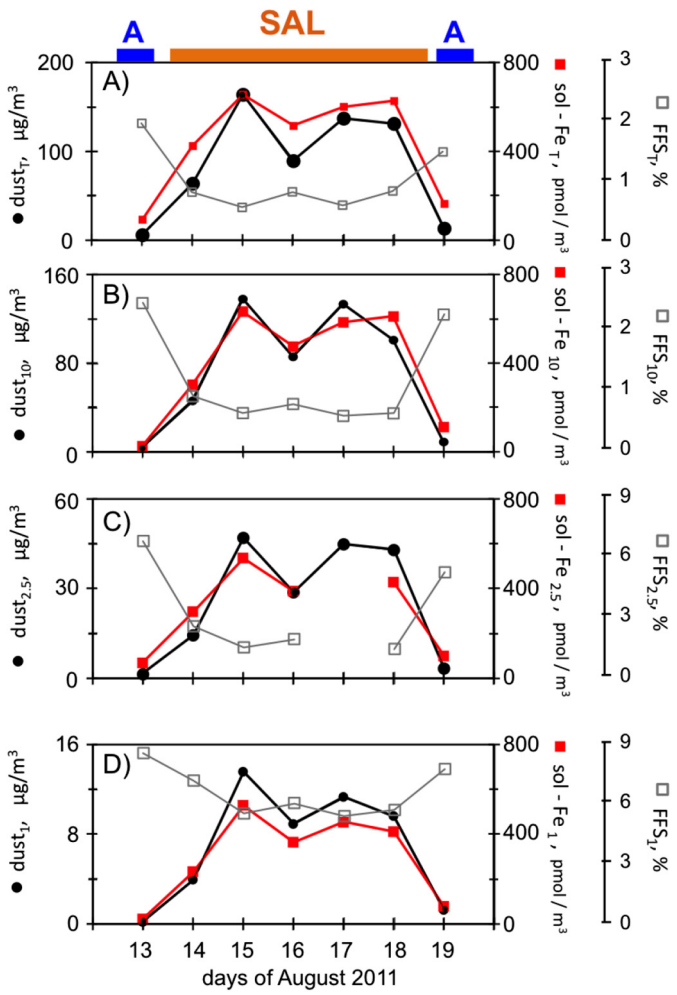

Fig. 4. Time series of dust, soluble (sol) Fe and Fractional Fe Solubility (FFS) in the four size fractions (total, sub 10, 2.5 and 1 μm). Samples collected in the Saharan Air Layer (SAL) and under Atlantic airflow conditions (A).

size. Approximately 90%, 75% and 70% of sol Fe occurs in the sub 10, 2.5 and 1 μm aerosols, respectively (Fig. S2 of the Supplementary Material); i.e. the 1–2.5 μm and 2.5–10 μm and >10 μm size fractions account for a minor fraction of soluble Fe (5, 15 and 10%, respectively) compared to the submicron fraction. Within the SAL, concentrations of sol-Fe_T ranged between 400 and 650 pmol/m^3, which mostly occurred in the submicron aerosols (Fig. 4). FFS versus dust concentrations in the sub 10 and 2.5 μm particles also showed the hyperbolic relationship (Fig. 5B–C) described above for the total aerosols (Fig. 5A). This hyperbolic relationship was smoothed in the submicron aerosols, which also showed a good FFS versus dust linear fitting (Fig. 5D) probable due to the higher Fe solubility in the submicron fraction and to the narrower variability range in the particle diameter in the submicron compared to the sub 10 and sub 2.5 μm ranges.

3.3. Sources of soluble Fe in the Saharan Air Layer

We paid special attention to the soluble Fe recorded in the SAL during 14–18 August 2011. In this section we analyse the relationship of soluble Fe with compounds that may trace the presence of clay minerals (Al; Journet et al., 2014), acids ($SO_4^{=}$, NH_4^+ and NO_3^-), fuel oil combustion elements (V; Sedwick et al., 2007) and biomass burning species (K; Paris et al., 2010). Additional data analysis is presented in section S3 of the Supplementary Material, which includes enrichment factors of the aerosol composition, with respect to the mean Earth crust, and correlations of sol Fe with Fe and size distribution of sol Fe.

Soluble Fe mostly occurred in the submicron fraction (~70%; Fig. S2). Our overall results suggest that soluble Fe in the submicron aerosols collected in the SAL is mostly associated with the dissolution of dust minerals rather than with combustion aerosols. In the submicron size range, we observe (i) a strong linear relationship between soluble Fe, Fe and Al (Figs. 6D and 7D) and (ii) a Fe to Al ratio (~0.55) similar to that we observe in the other size fractions (total, sub 10 and sub 2.5 μm), which is the typically observed in Saharan dust aerosols across the North Atlantic (Prospero et al., 2001; Sedwick et al., 2007). The V/Al ratio we observe (0.0015–0.0020 in all size ranges; Fig. 8) is similar to those reported for Saharan dust aerosols (Sedwick et al., 2007; Prospero et al., 2001) and for the upper continental crust (Mason, 1966; Taylor and McLennan, 1985), and significantly lower than that observed in fuel-combustion aerosols (Sedwick et al., 2007). The relatively constant V/Al ratios in the whole sol-Fe and FFS variability range values indicate a dominant influence of Saharan dust in the samples collected at Izaña (Fig. 8). Similarly, the high linearity in the K vs Al plots ($R^2 = 0.96$ to 0.99 in all PM_x cut sizes, not shown for the sake of brevity) and low K to Al ratios we observed (K-vs-Al slopes: 0.19 to 0.23, close to the 0.33 of the crust Earth; Mason, 1966) allows also to discard any significant influence of biomass burning aerosols, which typically occur in winter in the Sahel region (Nwofor et al.,

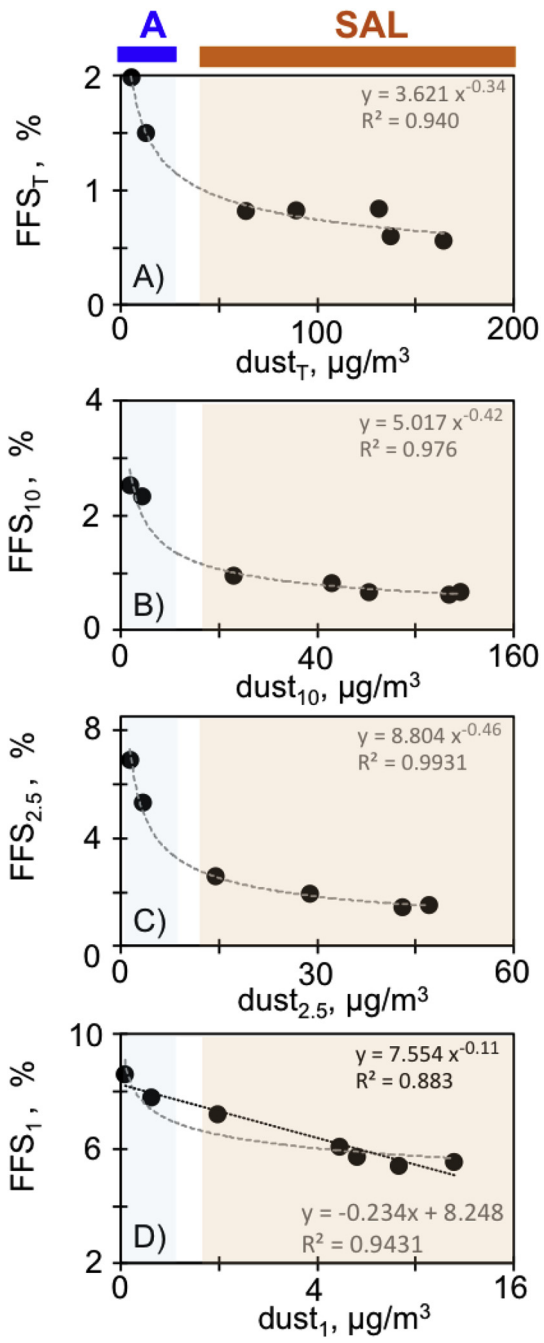

Fig. 5. Fractional Fe Solubility (FFS) versus dust concentrations in the four studied size fractions (total, sub 10, 2.5 and 1 µm). Data of samples collected under dust-free western North Atlantic (A) airflow conditions (13 and 19 Aug 2011) and in the Saharan Air Layer (SAL) (14–18 Aug 2011) are indicated with the blue and ochre shadow. Samples collected in the Saharan Air Layer (SAL) and under Atlantic airflow conditions (A). (For interpretation of the references to colour in this figure legend, the reader is referred to the web version of this article.)

2007) resulting in K to Al ratios of ~0.5 (Formenti et al., 2008; Paris et al., 2010). This analysis also indicates a predominant contribution of dust on soluble Fe in the total, sub 10 and sub 2.5 µm (Figs. 6A–C and 7A–C). These interpretations are also supported by the low values of the enrichment factors obtained for Fe, fuel oil combustion tracers (V and Ni) and other key (Cr, Cu, Zn or As) elements in the submicron and the other PM_x aerosols collected in the Saharan Air Layer (Section S3 and Table S2 of the Supplementary Material).

The correlation between sol-Fe, Fe and Al in the submicron aerosols (Figs. 6D and 7D) suggests that dissolution of Fe-bearing clays (e.g. illite, chlorites, smectite and palygorskite; Journet et al., 2014; Avila et al., 1997) may play a key role as source of sol-Fe in the submicron aerosols. The high linearity between sol Fe and Al suggests that the potential contribution of other Fe-bearing minerals, such as ferrihydrite and poorly crystalline Fe (Shi et al., 2009), Fe oxides (hematite and goethite, Arimoto et al., 2002; Lafon et al., 2004, 2006; Formenti et al., 2008; Shi et al., 2009) or magnetite (Lazaro et al., 2008), to sol Fe concentrations seems to keep a constant portion with respect to the amount of Al, only depend on particle size (Fig. 7). These results are consistent with previous studies. Shi et al. (2011b) observed that the size distribution of dissolved Fe was correlated with that of dissolved Al in Saharan dust soil samples, with the highest solubility for dust particles $\leq$ 0.6 µm. Journet et al. (2008) showed that Fe solubility of clays is higher than that of Fe oxides and suggested that clays could dominate Fe solubility in dust. Shi et al. (2009) showed that Fe oxides (frequently present as nano minerals onto clays; Reynolds et al., 2014) could be converted to labile Fe-rich nanoparticles by atmospheric processing.

3.4. Soluble Fe and dust processing in the Saharan Air Layer

Chemical composition and mass closure of PM_x in the SAL (Table 1) and the results of the enrichment factor analysis (section S3 and Table S2 of the Supplementary Material) indicates that the aerosol population in the SAL is dominated by desert dust enriched with nitrate and ammonium-sulphate linked to long range transport of these pollutants.

The solubility values we found in the fine atmospheric aerosol samples collected in the dusty Saharan Air Layer at Izaña are significantly higher than those observed in soil dust samples. For example, Shi et al. (2011a) found FFS values 0.2–0.8% at pH 4.7 for sub 2.5 µm dust particles collected in the soil of dust sources of Western Saharan, whereas (at the same pH) we observe FFS ~2% sub 2.5 µm aerosol dust particles collected in the SAL (Fig. 1). The difference is even higher with respect to the FFS of submicron dust aerosols, which show values ~6% in the SAL at Izaña even if measured at pH 8.13 (Fig. 5D), a pH value at which Fe solubility is minimum (Liu and Millero, 1999, 2002). This increase in solubility is typically attributed to the effects of aerosol aging by the atmospheric processing.

We assessed the potential involvement of acid processing by analysing sulphate, ammonium and nitrate data. As already described in previous studies, we found that in the SAL nitrate is mostly present as a non-ammonium salt coating supermicron (>1 µm) dust particles (Fig. 9C), whereas sulphate is present as a submicron ammonium salt (a-$SO_4^=$) and a non-ammonium salt (na-$SO_4^=$) – mostly occurring in the supermicron range – which in high concentrations have been linked to emissions of evaporite minerals (e.g. gypsum/anhydrite) in Saharan dry lakes – Chotts (Rodríguez et al., 2011). As usually observed in Izaña, concentrations of a-$SO_4^=$ and NO_3^- were higher under dusty SAL conditions than under dust-free western Atlantic airflows (Fig. 9). The correlation between FFS and the a-$SO_4^=$/dust ratio in submicron aerosols in the SAL (Fig. 10B) and the fact that the Fe / Al ratio does not change significantly (0.45–0.55) in those SAL samples (Fig. 10A), suggests that the presence of acids mixed with dust may have influenced solubility of Fe–bearing minerals. Our results are consistent with those of Ito and co-workers (Ito and Xu, 2014; Ito and Shi, 2016), who pointed out that dust Fe in the submicron range tend to be more easily processed – than in the supermicron range – due to ammonium-sulphate prompting a lower pH in this size range (<1 µm), even if nitrate is internally

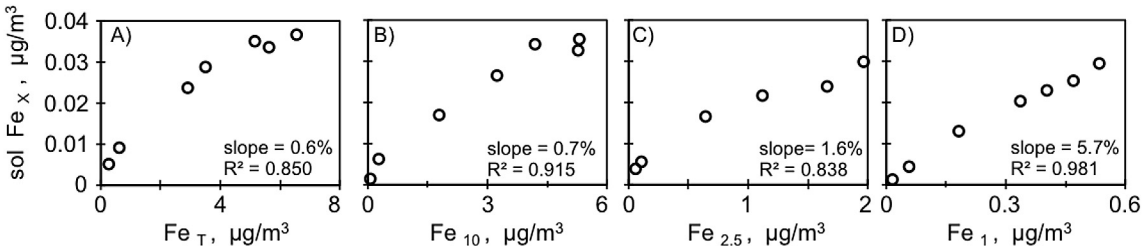

Fig. 6. Concentrations of soluble (sol) Fe versus Fe in the four studied size fractions (total and sub 10, 2.5 and 1 μm).

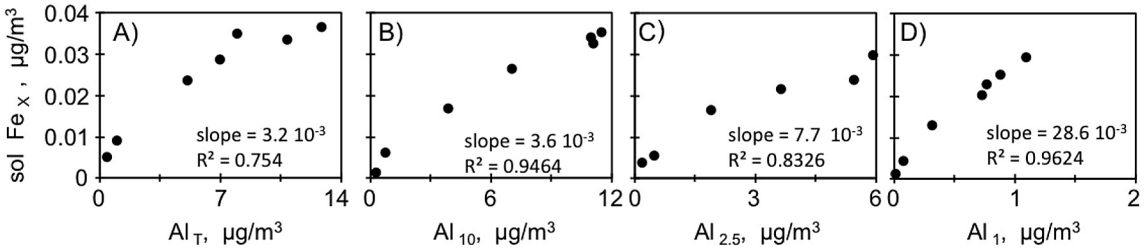

Fig. 7. Concentrations of soluble (sol) Fe versus Al in the four studied size fractions (total and sub 10, 2.5 and 1 μm).

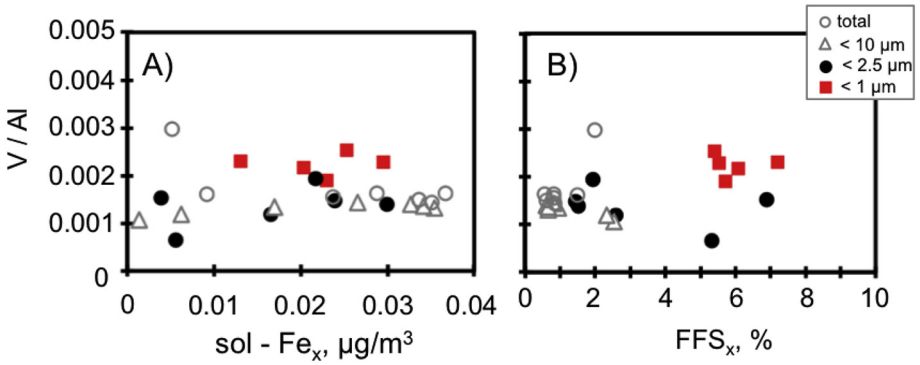

Fig. 8. Ratio Vanadium to Aluminium versus soluble (sol) Fe and versus Fractional Fe Solubility (FFS) in the four size fractions.

mixed with dust in the supermicron range. Ito and Feng (2010) assessed the impact of dust alkalinity on the acid mobilization of iron; they found that the buffering effect of alkaline minerals (e.g. carbonates) results in higher Fe solubility in the submicron than in the supermicron range and that it contributes to the inverse relationship between aerosol iron solubility and particle size. This is consistent with our observations, the supermicron fraction accounts for 96% of Ca (a fraction of which occurs as carbonate) and the 99% of nitrate, but only the 30% of soluble Fe. Long-term summer dust at Izaña has been connected to dust mobilization at the north of the ITCZ by the north-eastern (trade-Harmattan) winds (Rodríguez et al., 2015) in a scenario similar to that of the study event (Fig. 2C and F). The presence of acid pollutants in these north-eastern winds that result in dust emissions in inner Sahara may be linked to transport from Europe (Kallos et al., 2007), ship emissions in the Mediterranean (Marmer et al., 2009) and emissions of acid precursors (SO_2, NH_3 and NO_x) in industrial areas of Tunisia, Algeria and Morocco (Rodríguez et al., 2011). Back-trajectories of the study event support the latter scenario (Fig. 2F). Some studies have focused on dust aging during the trans-Atlantic transport. Our results suggest that acid processing of small dust particles may have occurred in a short time scale over the Sahara desert, i.e. before dust export to the Atlantic. Laboratory kinetic studies found that – at the pHs values typical of polluted acid conditions – dust undergoes an extremely fast Fe solubilisation in the first minutes and then the Fe dissolution rate slowdown along the next hours / days until reach a stable dissolution plateau (Shi et al., 2011b, 2011c). Additionally, in real atmospheric conditions, Fe dissolution will occur until acid is consumed.

Fig. 10C shows the FFS versus dust concentrations in size segregated dust samples collected in the SAL at Izaña. A high FFS is observed in aerosol dust populations dominated by small dust particles and characterised by low dust concentrations (e.g. FFS ~2% for 10–50 μg/m^3 of dust$_{2.5}$ and FFS ~6% for 3–13 μg/m^3 of dust$_1$; Fig. 10C). Such population (low concentrations of tiny dust particles) could be the result of trans-Atlantic dust transport in the SAL, during which large particles settle. These FFS values (~6%) for submicron dust aerosols we observed near North Africa are close to those registered along the East-to-West dust corridor over the Atlantic (e.g. 2–7%; Baker et al., 2006a). The dominance of soluble Fe by the submicron dust exported from North Africa in the SAL could explain why soluble Fe concentrations off the North African coast (at Izaña, Fig. 4) are close to those in the Caribbean (at Barbados, Trapp et al., 2010) during dust events, i.e. 300–600 pmol/m^3. Deposition of coarse and depleted in soluble Fe dust particles

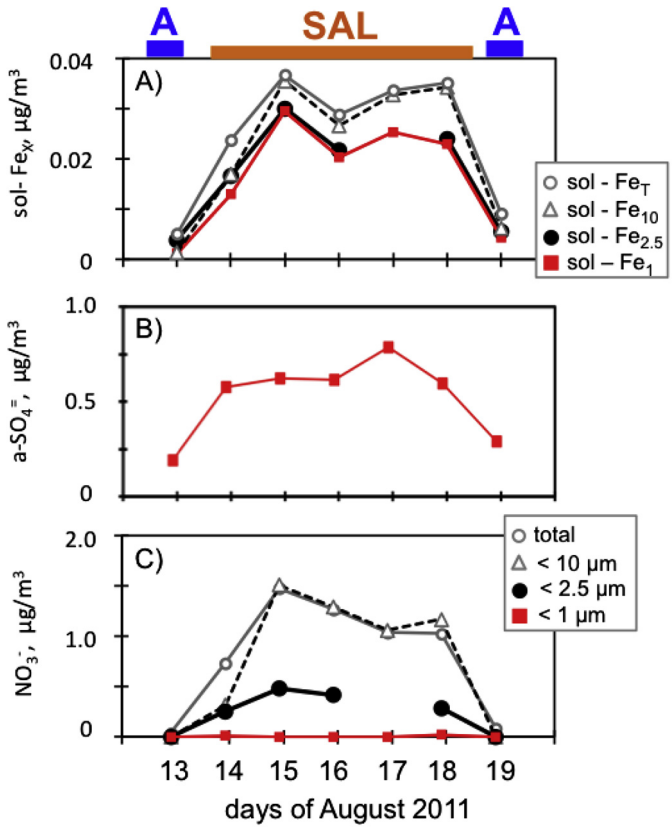

Fig. 9. Time series of soluble (sol) Fe, ammonium-sulphate and nitrate in the four size fractions. Samples collected in the Saharan Air Layer (SAL) and under Atlantic western airflow conditions (A).

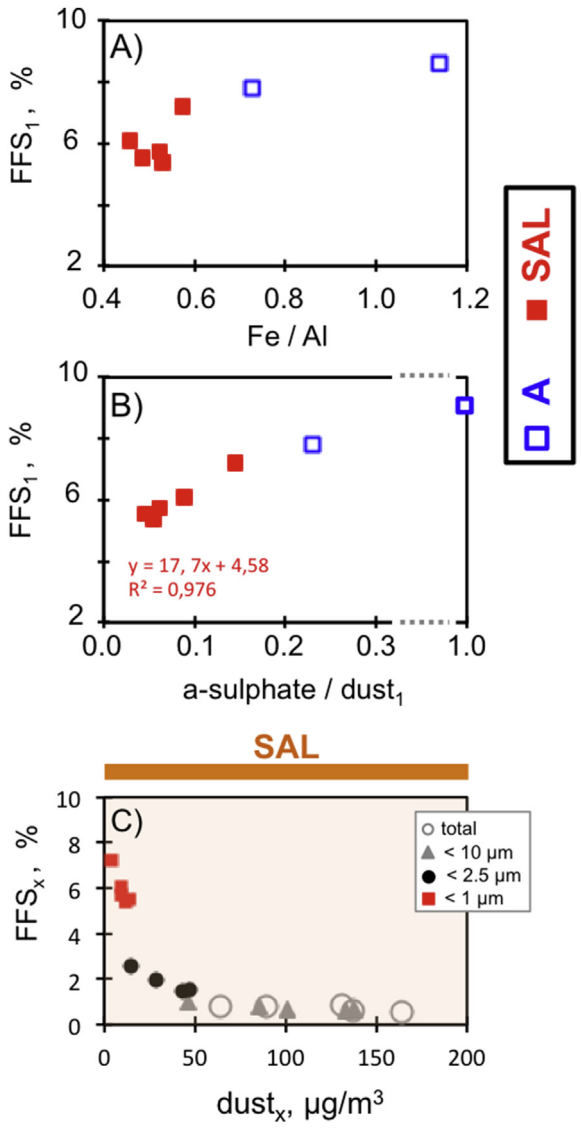

Fig. 10. Fractional Fe Solubility (FFS) versus Fe/Al (A) and a-sulphate/dust (B) ratio in the submicron aerosol collected in the Saharan Air Layer (SAL) and under Atlantic airflow conditions (A). (C) FFS versus dust concentrations in the four studied size fractions (total, sub 10, 2.5 and 1 µm) of samples collected 14–18 Aug 2011 in the SAL.

during the trans-Atlantic transport accounts for the lower dust$_T$ concentrations at Barbados (e.g. 10–50 µg/m^3) – compared to Izaña (50–300 µg/m^3) – and the consequent higher FFS$_T$ during dust events at Barbados (~2%) than in Izaña (~0.5%). Because of the dominant role of small dust particles in soluble Fe, FFS$_T$ at Barbados is within the range of that of FFS$_{2.5}$ at Izaña (~2%, Fig. 4C). Although this size dependence of Fe solubility in desert dust aerosols has been documented in a number of studies (cited above), it should be noted that Buck et al. (2010b) did not observed such trend and that Trapp et al. (2010) observed high FFS in the coarse range under the influence of biomass burning.

4. Conclusions

Huge amounts of desert dust particles are exported from the hyperarid Sahara to the North Atlantic in the Saharan Air Layer, a dust-laden corridor that expands from the North African coast to the Americas above the marine boundary layer. We found that ~70% of soluble Fe in the SAL off the North African coast is associated with the dissolution of submicron dust minerals—probably involving Fe-bearing clays – and that the Fractional Fe Solubility of submicron dust (~6%) is higher than that typically observed in submicron soil dust particles (<1%). The correlation of FFS with the ammonium-sulphate / dust ratio and the low variability in the Fe/Al ratio in the dust samples, suggests that the high FFS of submicron dust aerosols (compared to that of soil dust particles) may be related to acid processing of dust. Previous investigations focused on dust processing and changes in Fe solubility during the trans-Atlantic transport of dust. Our results indicate that (i) submicron dust exported off the coast of North Africa may have already experienced acid processing over the Sahara, i.e. before dust export to the Atlantic, and that (ii) export of soluble submicron Fe dust and deposition of coarse and depleted in soluble Fe dust particles during the trans-Atlantic transport may account for the observed variability in dust, soluble Fe and FFS. This idea should be corroborated in future experiments focused on comparing—by using homogenous sampling and analytical techniques – the features of Fe solubility in the "fresh aerosols (recently exported from the Sahara) directly collected in the SAL near North Africa" with those of the "aged aerosols collected in the marine boundary layer of the Caribbean" during specific trans-Atlantic events. This would allow the changes in Fe solubility during trans-Atlantic transport to be quantified.

Acknowledgements

This study is part of the project AEROATLAN – 2015-66229 -, funded by the Ministry of Economy and Competitiveness of Spain.

M.I. García holds a research grant – TESIS20120054 – co-funded by the Canarian Agency for Research, Innovation and Information Society and the European Social Fund. Chemical analysis, of the long-term chemical composition of aerosols GAW program at Izaña, are performed at the IDÆA-CSIC funded by AEMET. The authors are grateful to A. Stohl for providing FLEXTRA model and to J.J. Bustos (AEMET) for computing back trajectories. Daily, 1x1 degree, MODIS-Aqua data (level 3, collection 5.1) was downloaded from the Giovanni online data system, developed and maintained by the NASA GES DISC. We also thank the brotherhood of fishermen of La Punta del Hidalgo (Cofradía de Pescadores de La Punta del Hidalgo) for collecting offshore seawater and both the Research Support General Service (SEGAI) and the research group of Chemical Analysis Applied to the Industry, Environment and Agroalimentary Products of the University of La Laguna for the laboratory facilities.

Appendix A. Supplementary data

Supplementary data related to this article can be found at http://dx.doi.org/10.1016/j.atmosenv.2016.03.030.

References

Avila, A., Queralt-Mitjans, I., Alrcona, A., 1997. Mineralogical composition of African dust delivered by red rains over northeastern Spain. J. Geophys. Res. 102, 21977–21996.
Arimoto, R., Balsam, W., Schloesslin, C., 2002. Visible spectroscopy of aerosol particles collected on filters: iron-oxide minerals. Atmos. Environ. 36, 89–96.
Baker, A.R., Jickells, T.D., 2006. Mineral particle size as a control on aerosol iron solubility. Geophys. Res. Lett. 33, L17608.
Baker, A., French, M., Linge, K.L., 2006a. Trends in aerosol nutrient solubility along a west–east transect of the Saharan dust plume. Geophys. Res. Lett. 33, L07805.
Baker, A.R., Jickells, T.D., Witt, M., Linge, K.L., 2006b. Trends in the solubility of iron, aluminium, manganese and phosphorus in aerosol collected over the Atlantic Ocean. Mar. Chem. 98, 43–58.
Baker, A.R., Croot, P.L., 2010. Atmospheric and marine controls on aerosol iron solubility in seawater. Mar. Chem. 120, 4–13.
Bermejo-Barrera, P., Moreda-Pineiro, A., Moreda-Pineiro, J., Bermejo-Barrera, A., 1998. Usefulness of the chemical modification and multi-injection technique approaches in the electrothermal atomic absorption spectrometric determination of silver, arsenic, cadmium, chromium, mercury, nickel and lead in sea water. J. Anal. Atomic Spectrom. 13, 777–786.
Bopp, L., Kohfeld, K.E., Quere, C.L., Aumont, O., 2003. Dust impact on marine biota and atmospheric CO_2 during glacial periods. Paleoceanography 18, 1046.
Buck, C.S., Landing, W.M., Resing, J.A., Measures, C.I., 2010a. The solubility and deposition of aerosol Fe and other trace elements in the North Atlantic Ocean: observations from A16N CLIVAR/CO2 repeat hydrography section. Mar. Chem. 120.
Buck, C.S., Landing, W.M., Resing, J.A., 2010b. Particle size and aerosol iron solubility: a high- resolution analysis of Atlantic aerosols. Mar. Chem. 120, 14–24.
Chen, Y., Siefert, R.L., 2004. Seasonal and spatial distributions and dry deposition fluxes of atmospheric total and labile iron over the tropical and subtropical North Atlantic Ocean. J. Geophys. Res. 109, D09305.
Chen, Y., Street, J., Paytan, A., 2006. Comparison between pure-water- and seawatersoluble nutrient concentrations of aerosols from the Gulf of Aqaba. Mar. Chem. 101, 141–152.
De Baar, H.J.W., Boyd, P.W., Coale, K.H., Landry, M.R., Tsuda, A., 2005. Synthesis of 8 iron fertilization experiments: from the iron age to the age of enlightenment. J. Geophys. Res. 110, C09S16.
Fan, S.M., Moxim, W.J., Levy II, H., 2006. Aeolian input of bioavailable iron to the ocean. Geophys. Res. Lett. 33, L07602.
Formenti, P., Rajot, J.L., Desboeufs, K., Caquineau, S., Chevaillier, S., Nava, S., Gaudichet, A., Journet, E., Triquet, S., Alfaro, S., Chiari, M., Haywood, J., Coe, H., Highwood, E., 2008. Regional variability of the composition of mineral dust from western Africa: results from the AMMA SOP0/DABEX and DODO field campaigns. J. Geophys. Res. 113, D00C13.
Formenti, P., Schuetz, L., Balkanski, Y., Desboeufs, K., Ebert, M., Kandler, K., Petzold, A., Scheuvens, D., Weinbruch, S., Zhang, D., 2011. Recent progress in understanding physical and chemical properties of African and Asian mineral dust. Atmos. Chem. Phys. 11, 8231–8256.
Ginoux, P., Prospero, J.M., Torres, O., Chin, M., 2004. Long-term simulation of global dust distribution with the GOCART model: correlation with North Atlantic Oscillation. Environ. Model. Softw. 19, 113–128.
Ginoux, P., Prospero, J.M., Gill, T.E., Hsu, N.C., Zhao, M., 2012. Global-scale attribution of anthropogenic and natural dust sources and their emission rates based on MODIS deep blue aerosol products. Rev. Geophys. 50.
Hsu, N.C., Jeong, M.J., Bettenhausen, C., Sayer, A.M., Hansell, R., Seftor, C.S., Huang, J., Tsay, S.C., 2013. Enhanced deep blue aerosol retrieval algorithm: the second generation. J. Geophys. Res. 118.
Ito, A., Feng, Y., 2010. Role of dust alkalinity in acid mobilization of iron. Atmos. Chem. Phys. 10, 9237–9250. http://dx.doi.org/10.5194/acp-10-9237-2010.
Ito, A., Xu, L., 2014. Response of acid mobilization of iron-containing mineral dust to improvement of air quality projected in the future. Atmos. Chem. Phys. 14, 3441–3459.
Ito, A., Shi, Z., 2016. Delivery of anthropogenic bioavailable iron from mineral dust and combustion aerosols to the ocean. Atmos. Chem. Phys. 16, 85–99.
Jickells, T.D., An, Z.S., Andersen, K.K., Baker, A.R., Bergametti, G., Brooks, N., Cao, J.J., Boyd, P.W., Duce, R.A., Hunter, K.A., Kawahata, H., Kubilay, N., LaRoche, J., Liss, P.S., Mahowald, N., Prospero, J.M., Ridgwell, A.J., Tegen, I., Torres, R., 2005. Global iron connections between desert dust, ocean biogeochemistry, and climate. Science 308, 67–71.
Journet, E., Desboeufs, K.V., Caquineau, S., Colin, J.L., 2008. Mineralogy as a critical factor of dust iron solubility. Geophys. Res. Lett. 35, L07805.
Journet, E., Balkanski, Y., Harrison, S.P., 2014. A new data set of soil mineralogy for dust-cycle modeling. Atmos. Chem. Phys. 14, 3801–3816.
Kallos, G., Astitha, M., Katsafados, P., Spyrou, C., 2007. Long-range transport of Anthropogenically and naturally produced particulate matter in the Mediterranean and North Atlantic: current state of knowledge. J. Appl. Meteorol. Climatol. 46, 1230–1251.
Lafon, S., Rajot, J.L., Alfaro, S.C., Gaudichet, A., 2004. Quantification of iron oxides in desert aerosol. Atmos. Environ. 38, 1211–1218.
Lafon, S., Sokolik, I.N., Rajot, J.L., Caquineau, S., Gaudichet, A., 2006. Characterization of iron oxides in mineral dust aerosols: implications for light absorption. J. Geophys. Res. 111, D21207.
Lazaro, F.J., Gutierrez, L., Barron, V., Gelado, M.D., 2008. The speciation of iron in desert dust collected in Gran Canaria (Canary Islands): combined chemical, magnetic and optical analysis. Atmos. Environ. 42, 8987–8996.
Levy, R.C., Remer, L.A., Kleidman, R.G., Mattoo, S., Ichoku, C., Kahn, R., Eck, T.F., 2010. Global evaluation of the Collection 5 MODIS dark-target aerosol products over land. Atmos. Chem. Phys. 10, 10399–10420.
Liu, X., Millero, F.J., 1999. The solubility of iron in sodium chloride solutions. Geochim Cosmochim. Acta 63, 3487–3497.
Liu, X., Millero, F.J., 2002. The solubility of iron in seawater. Mar. Chem. 77, 43–54.
Marmer, E., Dentener, F., Aardenne, J.V., Cavalli, F., Vignati, E., Velchev, K., Hjorth, J., Boersma, F., Vinken, G., Mihalopoulos, N., Raes, F., 2009. What can we learn about ship emission inventories from measurements of air pollutants over the Mediterranean Sea? Atmos. Chem. Phys. 9, 6815–6831.
Martin, J.H., Fitzwater, S.E., 1988. Iron deficiency limits phytoplankton growth in the north- east Pacific subarctic. Nature 331, 341–343.
Mason, B., 1966. Principles of Geochemistry, third ed. John Wiley, New York.
Millero, F.J., Sohn, M.L., 1992. Chemical Oceanography. CRC Press, Boca Raton.
Nenes, A., Krom, M., Mihalopoulos, N., Van Cappellen, P., Shi, Z., Bougiatioti, A., Zarmpas, P., Herubt, B., 2011. Atmospheric acidification of mineral aerosols: a source of bioavailable phosphorus for the oceans. Atmos. Chem. Phys. 11, 6265–6272.
Nwofor, O.K., Chineke, T.C., Pinker, R.T., 2007. Seasonal characteristics of spectral aerosol optical properties at a sub-saharan site. Atmos. Res. 85, 38–51.
Paris, R., Desboeufs, K.V., Formenti, P., Nava, S., Chou, C., 2010. Chemical characterisation of iron in dust and biomass burning aerosols during AMMA-SOP0/DABEX: implication for iron solubility. Atmos. Chem. Phys. 10, 4273–4282.
Prospero, J.M., Carlson, T.N., 1972. Vertical and areal distribution of Saharan dust over the western Equatorial North Atlantic Ocean. J. Geophys. Res. 77, 5255–5265.
Prospero, J.M., Olmez, I., Ames, M., 2001. Al and Fe in $PM_{2.5}$ and PM_{10} suspended particles in south- central Florida: the impact of the long range transport of African mineral dust. Water Air Soil Pollut. 125, 291–317.
Raiswell, R., Benning, L.G., Tranter, M., Tulaczyk, S., 2008. Bioavailable iron in the Southern Ocean: the significance of the iceberg conveyor belt. Geochem. Trans. 9, 7.
Ramos, A.G., Cuevas, E., Perez, C., Baldasano, J.M., Coca, J., Redondo, A., Alonso-Perez, S., Bustos, J.J., Nickovic, S., April 13–18. 2008. Saharan dust and bloom of diazotrophic cyanobacteria in the NW African upwelling. In: European Geoscience Union General Assembly. Vienna.
Redmond, H.E., Dial, K.D., Thompson, J.E., 2010. Light scattering and absorption by wind-blown dust: theory, measurement and recent data. Aeolian Res. 2, 5–26.
Reynolds, R.L., Cattle, R.S., Moskowitz, B.M., Goldstein, H.L., Yauk, K., Flagg, C.B., Berquo, T.S., Kokaly, R.F., Morman, S., Breit, G.N., 2014. Iron oxide minerals in dust of the Red Dawn event in eastern Australia, September 2009. Aeolian Res. 15, 1–13.
Ridgwell, A.J., Watson, A.J., 2002. Feedback between aeolian dust, climate and atmospheric CO_2 in glacial time. Paleoceanography 17, 1059.
Rodrıguez, S., Torres, C., Guerra, J.C., Cuevas, E., 2004. Transport pathways of ozone to marine and free-troposphere sites in Tenerife, Canary Islands. Atmos. Environ. 38, 4733–4747.
Rodríguez, S., Alastuey, A., Alonso-Pérez, S., Querol, X., Cuevas, E., Abreu-Afonso, J., Viana, M., Pandolfi, M., de la Rosa, J., 2011. Transport of desert dust mixed with North African industrial pollutants in the subtropical Saharan Air Layer. Atmos. Chem. Phys. 11, 6663–6685.
Rodríguez, S., Alastuey, A., Querol, X., 2012. A review of methods for long term in situ characterization of aerosol dust. Aeolian Res. 6, 55–74.
Rodríguez, S., Cuevas, E., Prospero, J.M., Alastuey, A., Querol, X., López-Solano, J., García, M.I., Alonso-Pérez, S., 2015. Modulation of Saharan dust export by the North African dipole. Atmos. Chem. Phys. 15, 7471–7486.

Rothlisberger, R., Bigler, M., Wolff, E.W., Joos, F., Monnin, E., Hutterli, M.A., 2004. Ice core evidence for the extent of past atmospheric CO2 change due to iron fertilisation. Geophys. Res. Lett. 31, L16207. http://dx.doi.org/10.1029/2004GL020338.

Schulz, M., Prospero, J.M., Baker, A.R., Dentener, F., Ickes, L., Liss, P.S., Mahowald, N.M., Nickovic, S., Perez Garcia-Pando, C., Rodriguez, S., Sarin, M., Tegen, I., Duce, R.A., 2012. Atmospheric transport and deposition of Mineral dust to the ocean: implications for research needs. Environ. Sci. Technol. 46, 10390–10404.

Sedwick, P.N., Sholkovitz, E.R., Church, T.M., 2007. Impact of anthropogenic combustion emissions on the fractional solubility of aerosol iron: evidence from the Sargasso Sea. Geochem. Geophys. Geosys. 8, Q10Q06.

Shi, Z., Krom, M.D., Bonneville, S., Baker, A.R., Jickells, T.D., Benning, L.G., 2009. Formation of iron nanoparticles and increase in iron reactivity in the mineral dust during simulated cloud processing. Environ. Sci. Technol. 43, 6592–6596.

Shi, Z., Krom, M.D., Bonneville, S., Baker, A.R., Bristow, C., Drake, N., Mann, G., Carslaw, K., McQuaid, J.B., Jickells, T., Benning, L.G., 2011a. Influence of chemical weathering and aging of iron oxides on the potential iron solubility of Saharan dust during simulated atmospheric processing. Glob. Biogeochem. Cycles 25, GB2010.

Shi, Z.B., Woodhouse, M.T., Carslaw, K.S., Krom, M.D., Mann, G.W., Baker, A.R., Savov, I., Fones, G.R., Brooks, B., Drake, N., Jickells, T.D., Benning, L.G., 2011b. Minor effect of physical size sorting on iron solubility of transported mineral dust. Atmos. Chem. Phys. 11, 8459–8469.

Shi, Z., Bonneville, S., Krom, M.D., Carslaw, K.S., Jickells, T.D., Baker, A.R., Benning, L.G., 2011c. Iron dissolution kinetics of mineral dust at low pH during simulated atmospheric processing. Atmos. Chem. Phys. 11, 995–1007.

Shi, Z., Krom, M.D., Jickells, T.D., Bonneville, S., Carslaw, K.S., Mihalopoulos, N., Baker, A.R., Benning, L.G., 2012. Impacts on iron solubility in the mineral dust by processes in the source region and the atmosphere: a review. Aeolian Res. 5, 21–42.

Sholkovitz, E.R., Sedwick, P.N., Church, T.M., Baker, A.R., Powell, C.F., 2012. Fractional solubility of aerosol iron: synthesis of a global-scale data set. Geochim. Cosmochim. Acta 89, 173–189.

Stohl, A., 1999. The FLEXTRA Trajectory model. Version 3.0 User Guide. Lehrstuhl fur Bioklimatologie und Immissionsforschung. University of Munich.

Taylor, S.R., McLennan, S.M., 1985. The Continental Crust: Its Composition and Evolution. Blackwell Sci., Oxford, U.K, p. 312.

Theodosi, C., Markaki, Z., Mihalopoulos, N., 2010. Iron speciation, solubility and temporal variability in wet and dry deposition in the Eastern Mediterranean. Mar. Chem. 120, 100–107.

Trapp, M.J., Millero, F.J., Prospero, J.M., 2010. Trends in the solubility of iron in dust-dominated aerosols in the equatorial Atlantic trade winds: importance of iron speciation and sources. Geochem. Geophys. Geosys. 11, 1–22.

Tsamalis, C., Chédin, A., Pelon, J., Capelle, V., 2013. The seasonal vertical distribution of the Saharan Air Layer and its modulation by the wind. Atmos. Chem. Phys. 13, 11235–11257.

Wagener, T., Guieu, C., Leblond, N., 2010. Effects of dust deposition on iron cycle in the surface Mediterranean Sea: results from a mesocosm seeding experiment. Biogeosci 7, 2769– 3781.